Real Space Trajectory of the Ultrafast Magnetization Dynamics in Ferromagnetic Metals

M. Vomir, L. H. F. Andrade, L. Guidoni, E. Beaurepaire, and J.-Y. Bigot*

Institut de Physique et Chimie des Matériaux de Strasbourg, Unité Mixte 7504 CNRS, Université Louis Pasteur BP. 43, 23 rue du Loess, 67034 Strasbourg Cedex, France

(Received 25 November 2004; published 14 June 2005)

We have measured the real space trajectory of the ultrafast magnetization dynamics in ferromagnetic metals induced by femtosecond optical pulses. Our approach allows the observation of the initial change of the modulus and orientation of the magnetization, occurring within a few hundreds of femtoseconds, as well as its subsequent precession and damping around the effective field. The role of the magnetocrystalline anisotropy shows up in the magnetization reorientation occurring during the electron-lattice relaxation. In addition, we propose a model which takes into account the initial demagnetization in the Bloch formalism describing the magnetization dynamics.

DOI: 10.1103/PhysRevLett.94.237601 PACS numbers: 76.50.+g, 75.70.Ak, 78.20.Ls, 78.47.+p

The search for efficient devices used in magnetic data processing and storage requires working along two major directions: the investigation of nanostructured materials as well as the search for systems having an ultrafast magnetic response. Recently, this second requirement has made significant progress as it has been shown that the magnetic response can be modified and monitored using femtosecond optical pulses [1–8]. Indeed, different approaches using ultrafast time resolved techniques have demonstrated an initial ultrafast demagnetization occurring within the first few hundreds of femtoseconds following the excitation of the magnetic material. A detailed investigation of the initial step leading to the demagnetization has shown, using pulses of 20 fs duration, that it occurs within the thermalization time of the electrons, i.e., $\sim$60 fs in the case of CoPt ferromagnetic thin films [9]. Some questions are, however, still open regarding the magnetization dynamics. In particular, the mechanisms involved in the demagnetization process are not yet identified. In addition, it is important to understand the dynamics leading to a change in the effective field which can initiate a precession motion. In this Letter we describe an experimental procedure allowing to address such ultrafast dynamical behavior using the time resolved Kerr polarimetric technique. The results obtained in cobalt thin films allow us to obtain information on the influence of the time dependent anisotropy on the overall magnetization dynamics. We propose a dynamical model based on the Bloch formalism, with a time dependent effective field, to account for the initial demagnetization and subsequent precession and damping.

From a fundamental point of view, this method of investigating the real space trajectory of the magnetization presents several advantages as compared to manipulating the magnetization with radio-frequency modulated magnetic fields. First, the temporal resolution is in principle limited by the optical pulse duration (femtosecond regime); second, it can easily be transposed to confocal optical geometries allowing a local probing of the magnetization dynamics on a scale typically limited by diffraction ($\geq$500 nm). Finally, it is a powerful way to study the influence of time dependent quantities like the anisotropy or the exchange interaction.

One can take advantage of the optically induced demagnetization process [1] to launch a motion of precession of the magnetization around the effective magnetic field. This is the temporal analogous of the ferromagnetic resonance observed in the frequency domain which is induced by radio-frequency magnetic field [10]. The use of optical methods has been reported earlier in the study of the coherent magnetization rotation induced optically in an exchange coupled NiFe/NiO bilayer [3] as well as the all-optical probing of spin waves in ferromagnetic nickel and permalloy [11]. We focus on the real space trajectory of the magnetization vector. It allows the onset of the precession motion to be clearly observed, which, during the first hundreds of femtoseconds, begins in the plane defined by the initial static magnetization and the external static magnetic field. This approach of following the temporal evolution and the full space trajectory of the magnetization modified by femtosecond pulses raises interesting questions regarding the theoretical description of the dynamics. Clearly, one cannot simply consider Landau-Lifshitz-Gilbert macroscopic equations since the modulus is not conserved during the overall process. We discuss here these aspects, proposing a time dependent version of the Bloch equations including a source term which modifies the modulus of the magnetization.

The time resolved Kerr measurements were performed using a femtosecond laser setup consisting of an amplified Ti:sapphire laser centered at 790 nm operating at 2.5 kHz. The pulse duration is 120 fs. For noise discrimination purposes occurring at short temporal delays, the probe and pump pulses are, respectively, at 790 and 395 nm. The diameter of the focused pump and probe are 100 and 30 μm, respectively. The maximum energy density of the pump pulse is 0.5 mJ/cm^2. In general, the static magnetization can be retrieved for a given angle of the probe impinging on the sample via the analysis of the polar,

longitudinal, and transverse components of the magneto-optical Kerr signals [12,13]. We implemented a dynamical version of this ellipsometric technique by measuring the time dependent polar, longitudinal, and transverse components. The Kerr rotations (and Kerr ellipticities) are analyzed with a polarization bridge and detected with a lock-in amplifier. In addition, we measure the transmission and reflectivity of the probe beam. The dynamical measurements are performed in the presence of a variable static magnetic field up to 3.2×10^5 A/m.

The cobalt samples, grown at 500 °C, are obtained by molecular beam epitaxy on (0001) oriented sapphire substrates. The growth axis lies along the (0001) axis of sapphire resulting in a hexagonal compact crystalline phase [14]. However, an inhomogeneous anisotropy remains in the plane of the sample as observed from static Kerr measurements. Although we also studied nickel and permalloy films on various substrates, hereafter we are considering the dynamics obtained from a 16 nm Co thin film on sapphire.

In the following, we chose a three-dimensional set of axes in which the Oy and Oz axes lie in the plane of the sample while xOy refers to the plane of incidence of the pump and probe beams. Therefore, the directions Ox, Oy, Oz correspond, respectively, to the polar (Pol), longitudinal (Long), and transverse (Trans) magneto-optical signals. The angle θ between the external field $\mathbf{H}_0$ and the Oz axis is kept constant at 90°. The angle φ between $\mathbf{H}_0$ and Ox can be varied. In order to retrieve the polar and longitudinal components of the magnetization, we measure the polarimetric signals$S(\varphi)$ for two complementary angles φ [15]: $\mathrm{Pol} = [S(\varphi) + S(-\varphi)]/2$ or $\mathrm{Pol} = [S(\varphi) - S(\pi - \varphi)]/2$ and $\mathrm{Long} = [S(\varphi) - S(-\varphi)]/2$ or $\mathrm{Long} = [S(\varphi) + S(\pi - \varphi)]/2$. The transverse signal Trans is obtained directly from the reflectivity R without polarization analysis and removing the nonmagnetic contribution, that is $\mathrm{Trans} = [R(\varphi) - R(\pi - \varphi)]/2$. Let us emphasize that this measurement procedure requires the incident probe beam to be p polarized [13,16]. In addition, we checked the consistency of the results by using simultaneously two probe beams having different angles of incidence of, respectively, 52° and 3°. The dynamics of the polar and longitudinal components, as a function of the pump-probe delay t, are defined as: $\Delta\mathrm{Pol}(t) = [\mathrm{Pol}(t) - \mathrm{Pol}_{\mathrm{stat}}]/\mathrm{Pol}_{\mathrm{stat}}$ and $\Delta\mathrm{Long}(t) = [\mathrm{Long}(t) - \mathrm{Long}_{\mathrm{stat}}]/\mathrm{Long}_{\mathrm{stat}}$, where $\mathrm{Pol}_{\mathrm{stat}}$ ($\mathrm{Long}_{\mathrm{stat}}$) refers to the static polar (longitudinal) signal without pump pulse. The definition of the relative variation of the transverse component $\Delta\mathrm{Trans}(t)$ is different since its static value is zero because the initial magnetization is set in the plane of incidence ($\theta = 90°$). During the precession motion, a transverse component shows up as $\mathbf{M}(t)$ rotates around the effective field. Therefore, we normalized the transverse component to its static value at saturation when $\mathbf{H}_0$ is parallel to Oz ($\theta = 0$): $\Delta\mathrm{Trans}(t) = \mathrm{Trans}(t)/\mathrm{Trans}_{\mathrm{stat}}$. Although we performed systematic measurements for different angles φ, in the following we will mainly focus on the angles $\varphi = \pm 15°$ and 165°.

We first checked the consistency of the measurement procedure by studying the precession period as a function of $\mathbf{H}_0$, as shown in Fig. 1(a). Two main features can be distinguished. The first one which will be detailed in the rest of this Letter is an initial ultrafast decrease of the magnetization followed by a partial recovery during the first picoseconds. The second feature is the oscillatory behavior and damping associated to the motion of precession. As expected from the ferromagnetic resonance, the frequency of the oscillations increase when the field $\mathbf{H}_0$ increases [bars in Fig. 1(c)]. This behavior is similar to the results reported in NiFe/NiO bilayer [3], ferromagnetic nickel, and permalloy [11] or GdFeCo structures [17].

Let us now focus on the trajectory of the magnetization. The detailed motion of precession along the three coordinate axes is displayed in Fig. 2 for short [2(a)–2(c)] and long [2(d)–2(f)] temporal delays. For short delays, it can be seen that both the polar and longitudinal signals decrease within the pump pulse excitation, while the transverse component does not show any ultrafast variation. This proves that the magnetization vector remains in the xOy plane during the demagnetization process. It is accompanied by a reorientation in the xOy plane while the modulus partially recovers, a process which occurs during the electron and spin relaxation to the lattice. After the

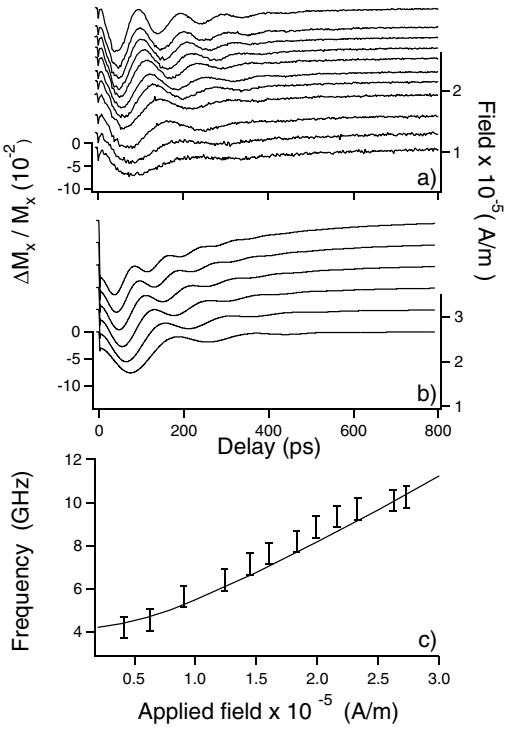

FIG. 1. Experimental (a) and simulated (b) time dependent differential magnetization for various external static fields H_0 on a 16 nm Co/Al_2O_3 film. (c) Corresponding precession frequencies vs H_0: experiment (bars) and model (full curve). For convenient reading, in (a) and (b) a vertical offset has been introduced.

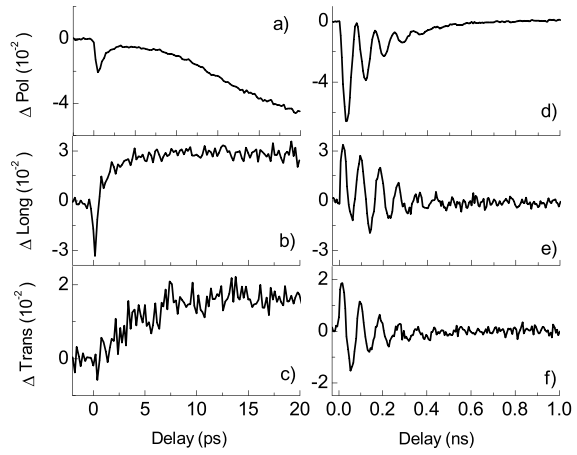

FIG. 2. Polar, longitudinal, and transverse differential Kerr signals for short (a)–(c) and long pump-probe delays (d)–(f).

partial recovery of the magnetization, the onset of the precession can be seen in all three directions as clearly seen for long delays in Figs. 2(d)–2(f).

The method allows us to obtain fine details of the magnetization dynamics as seen in the trajectory plots (ΔPol vs ΔLong; ΔTrans vs ΔPol; ΔTrans vs ΔLong). In the polar/longitudinal plane (xOy) the initial motion consists in a decrease of the magnetization modulus as well as a rotation in this plane. The magnetization trajectory follows a complex path where the modulus and the angle of $\mathbf{M}(t)$ are time dependent as well as the orientation of the effective field. The detailed behavior of this modulus/rotation trajectory for short delays is displayed in Fig. 3(d). Indeed, the fact that both ΔPol and ΔLong components decrease, means that the modulus first decreases. In order to have a correspondence between these various steps in the temporal evolution of the magnetization and the time dependent temperature variation of the sample, we plotted in Fig. 3(e) the differential transmission

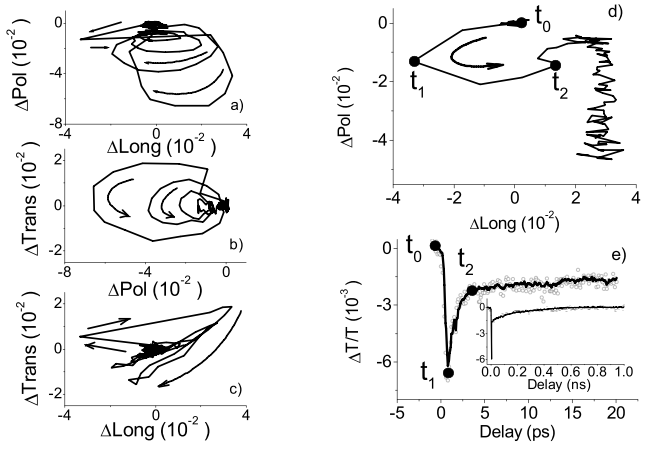

FIG. 3. (a)–(c) Projections of the magnetization trajectory; (d) the same as (a) at short temporal delays and (e) differential transmission (full curve) and longitudinal signal (open circles) rescaled for $\mathbf{H}_0 \parallel Oy$.

$\Delta T/T$. We also superimposed the dynamics of the rescaled longitudinal Kerr signal for an external field $\mathbf{H}_0$ set in the plane of the sample along the y axis. Both quantities follow the same dynamics as no precession occurs when $\mathbf{H}_0$ is parallel to the y axis. To clarify the correspondence between the trajectory and the temporal evolution of $\mathbf{M}(t)$, we marked in Figs. 3(d) and 3(e) by t_0, t_1, and t_2, some important steps of the dynamics discussed in the following paragraph. Different steps in the electron/spin dynamics are driving the trajectory of the magnetization. As it is well known in metals excited by femtosecond optical pulses, initially the nonthermal electron gas thermalizes within $\sim$100 fs [$t < t_1$ in Fig. 3(e)] due to electron-electron scattering. Then, the hot electron gas (which is responsible here for the initial demagnetization) cools down by exchanging energy with the lattice which simultaneously heats up. This process occurs within a few picoseconds [$t < t_2$ in Fig. 3(e)] and depends on the density of laser excitation. The next step ($t \gg t_2$) corresponds to a heat diffusion in the environment, that is a lateral diffusion in the metal and a perpendicular heat transfer to the substrate. This process occurs within a fraction of a nanosecond and depends on the heat diffusivity of both systems (metal and substrate). We interpret the initial magnetization dynamics in Fig. 3(d) as the result of the demagnetization induced by the pump pulse when the electron gas heats up ($t < t_1$), as well as a change of the magnetocrystalline anisotropy which occurs while the electron-lattice equilibrium takes place ($t < t_2$). At the end of this process, the magnetization vector being out of equilibrium, it will start its precession motion displayed for longer delays in Fig. 2. Later on, when the heat dissipates to the environment ($t \gg t_2$), the precession damps while the magnetization recovers to its initial value in a time scale similar to the differential transmission signal. The corresponding relaxation time $T_1 = 300$ ps is obtained from the long delay behavior of both $\Delta T/T$ and $\Delta M/M$ ($\mathbf{H}_0 \parallel Oy$). Later on, when the heat dissipates to the environment, the effective field goes back to its initial static value.

In order to model the precession dynamics induced by femtosecond optical pulses, one cannot simply use the Landau-Lifschitz-Gilbert equations, which do not include the ultrafast demagnetization. In addition, one has to take into account a dynamical change of the magnetization modulus which obviously is not conserved during the overall process. We propose an alternative way that combines the motion of precession using classical Bloch equations and a time dependent source term $P(t)\mathbf{M}(t)$, which induces the demagnetization, where $P(t)$ corresponds to the envelope of the pump pulse

$$\frac{d\mathbf{M}(t)}{dt} = \gamma \mathbf{M}(t) \times \mathbf{H}_{\text{eff}}(t) - \left[\frac{d\mathbf{M}(t)}{dt}\right]_{\text{relax}} - P(t)\mathbf{M}(t), \tag{1}$$

where $\mathbf{H}_{\text{eff}}(t)$ stands for the time dependent effective field resulting from the external field $\mathbf{H}_0$ as well as the shape

$\mathbf{H}_d(t)$ and $\mathbf{H}_{\text{anis}}(t)$ magnetocrystalline anisotropies. $[d\mathbf{M}/dt]_{\text{relax}}$ corresponds to the damping, which in the Bloch formalism can be accounted for using the two phenomenological constants T_1 and T_2. Let us emphasize that this procedure of incorporating a source term is consistent with a decrease of the magnetization modulus at short delays, which is proportional to $P(t)$, since Eq. (1) leads to $d|\mathbf{M}^2|/dt = -2P(t)|\mathbf{M}|^2$. It is important to stress that, in general, for ferromagnets, the intrinsic dephasing time T_2 of the magnetization is very long (the spins are correlated and cannot easily dephase with respect to one another) [18]. In contrast, the damping time T_1, which can be inferred from the line shape of the ferromagnetic resonance spectra, is such that $T_1 \ll T_2$. It is therefore sufficient to use one damping parameter α and the dynamics is well described equivalently by a Landau-Lifschitz-Gilbert model, provided that the modulus is conserved. In the optically induced FMR, both the nonconservation of the magnetization modulus and the relaxation dynamics of the temperature do not allow such description. Indeed, the dephasing and lifetime are driven by the relaxation to the environment (heat diffusion), i.e., $\sim$300 ps in the present experiment. In Fig. 1(b) the magnetization dynamics of a cobalt film, using Eq. (1), is displayed for different applied static fields. The corresponding variation of the precession period is shown by the full line in Fig. 1(c). The main characteristics of the demagnetization and precession are reproduced as compared with Figs. 1(a) and 1(c) (bars). The following parameters have been used: $\gamma = 2.4 \times 10^5$ A^{-1} m s^{-1}; $H_{d,x} = 4\pi M_x$, $H_{d,y} = H_{d,z} = 0$; $H_{\text{anis},z} = 0$, $H_{\text{anis},y} = 2D_yM_y(D_y = 0.075)$; $H_{\text{anis},x} = 2D_xM_x(D_x = 0.5)$; $T_1 = T_2 = 0.3 \times 10^{-9}$ s. The source term $P(t)$ is a Gaussian with a temporal width of 200 fs. The static magnetization at saturation is 1.37×10^6 A m^{-1}. The preceding approach can be complicated at will by incorporating a more sophisticated time dependent behavior. For example, Eq. (1) can be solved simultaneously with a two-temperature model representing the electron/spin $[T_e(t)]$ and lattice $[T_{\text{lat}}(t)]$ temperatures. The time dependent magnetocrystalline anisotropy can then be considered via the variation of the lattice temperature $T_{\text{lat}}(t)$. We investigated such dependency in various materials (Ni, Co hcp, permalloy) and the results will be reported elsewhere.

In conclusion, we have measured the real space trajectory of the magnetization in ferromagnetic thin films. It is a new approach that takes advantage of the flexibility of the magneto-optical polarimetric analysis to retrieve the modulus and orientation of the magnetization vector with femtosecond temporal resolution. It is particularly well suited to study the change of the anisotropy associated with the dynamical heating of the lattice, which is of great interest in the context of the current investigation of precessional switching in ferromagnetic nanostructures. In addition it provides useful information on the subsequent motion of precession and damping. This approach, which is powerful to understand the early dynamics leading to the precession motion, is complementary to pulsed magnetic field techniques [19,20] which are better suited for long delays (study of precession damping) owing to the longer pulse rise time or jitter (a few tens of picoseconds).

L. H. F. A., on leave from CDTN/CNEN-Belo Horizonte Brazil, would like to thank CNRS for financial support. This work is supported in part by the EU project DYNAMICS. We are grateful to M. Albrecht and J. Arabski for their technical support.

*Electronic address: bigot@ipcms.u-strasbg.fr

[1] E. Beaurepaire, J.-C. Merle, A. Daunois, and J.-Y. Bigot, Phys. Rev. Lett. **76**, 4250 (1996).
[2] E. Beaurepaire, M. Maret, V. Halté, J.-C. Merle, A. Daunois, and J.-Y. Bigot, Phys. Rev. B **58**, 12 134 (1998).
[3] G. Ju, A. V. Nurmikko, R. F. C. Farrow, R. F. Marks, M. J. Carey, and B. A. Gurney, Phys. Rev. Lett. **82**, 3705 (1999).
[4] J. Hohlfeld, E. Matthias, R. Knorren, and K. H. Bennemann, Phys. Rev. Lett. **78**, 4861 (1997).
[5] B. Koopmans, M. van Kampen, J. T. Kohlhepp, and W. J. M. de Jonge, Phys. Rev. Lett. **85**, 844 (2000).
[6] A. Scholl, L. Baumgarten, R. Jacquemin, and W. Eberhardt, Phys. Rev. Lett. **79**, 5146 (1997).
[7] M. Aeschlimann, M. Bauer, S. Pawlik, W. Weber, R. Burgermeister, D. Oberli, and H. C. Siegmann, Phys. Rev. Lett. **79**, 5158 (1997).
[8] A. V. Kimel, A. Kirilyuk, A. Tsvetkov, R. V. Pisarev, and Th. Rasing, Nature (London) **429**, 850 (2004).
[9] L. Guidoni, E. Beaurepaire, and J.-Y. Bigot, Phys. Rev. Lett. **89**, 017401 (2002).
[10] J. H. E. Griffiths, Nature (London) **158**, 670 (1946).
[11] M. van Kampen, C. Jozsa, J. T. Kohlhepp, P. LeClair, L. Lagae, W. J. M. de Jonge, and B. Koopmans, Phys. Rev. Lett. **88**, 227201 (2002).
[12] J. Zak, E. R. Moog, C. Liu, and S. D. Bader, Phys. Rev. B **43**, 6423 (1991).
[13] M. E. Brubaker, E. R. Moog, C. H. Sowers, J. Zak, and S. D. Bader, J. Magn. Magn. Mater. **103**, L7 (1992).
[14] H. A. M. de Gronckel, P. J. H. Bloemen, E. A. M. van Alphen, and W. J. M. de Jonge, Phys. Rev. B **49**, 11 327 (1994).
[15] H. F. Ding, S. Pütter, H. P. Oepen, and J. Kirschner, J. Magn. Magn. Mater. **212**, L5 (2000).
[16] C. Penfold, R. T. Collins, A. P. B. Tufaile, and Y. Souche, J. Magn. Magn. Mater. **242**, 964 (2002).
[17] A. Tsukamoto, K. Nakagawa, A. Itoh, A. Kimel, A. Tsvetkov, H. Awano, N. Ohta, A. Kirilyuk, and Th. Rasing, IEEE Trans. Magn. **40**, 2543 (2004).
[18] A. I. Akhiezer, V. G. Bar'yakhtar, and S. V. Peletminskii, *Spin Waves* (North-Holland, Amsterdam, 1968), Chap. 7.
[19] T. J. Silva, P. Kabos, and M. R. Pufall, Appl. Phys. Lett. **81**, 2205 (2002).
[20] Th. Gerrits, T. J. Silva, J. P. Nibarger, and Th. Rasing, J. Appl. Phys. **96**, 6023 (2004).